

# **Archive ouverte UNIGE**

https://archive-ouverte.unige.ch

Article scientifique

Article

1983

**Published version** 

**Open Access** 

This is the published version of the publication, made available in accordance with the publisher's policy.

Anisotropy of magnetic susceptibility and magmatic structures in the Guérande Granite Massif (France)

Guillet, Philippe Dario Louis; Bouchez, Jean-Luc; Wagner, Jean-Jacques

## How to cite

GUILLET, Philippe Dario Louis, BOUCHEZ, Jean-Luc, WAGNER, Jean-Jacques. Anisotropy of magnetic susceptibility and magmatic structures in the Guérande Granite Massif (France). In: Tectonics, 1983, vol. 2, n° 5, p. 419–429. doi: 10.1029/TC002i005p00419

This publication URL: <a href="https://archive-ouverte.unige.ch/unige:164495">https://archive-ouverte.unige.ch/unige:164495</a>

Publication DOI: <u>10.1029/TC002i005p00419</u>

© This document is protected by copyright. Please refer to copyright holder(s) for terms of use.

TECTONICS, VOL. 2, NO. 5, PAGES 419-429, OCTOBER 1983

France (Passif Course). Remographe. Structurale. Palemajuelisa.

ANISOTROPY OF MAGNETIC SUSCEPTIBILITY AND MAGMATIC STRUCTURES
IN THE GUERANDE GRANITE MASSIF (FRANCE)

Philippe Guillet and Jean-Luc Bouchez

Laboratoire de Tectonophysique, Université de Nantes

Jean-Jacques Wagner

Laboratoire de Pétrophysique, Université de Genève

multidisciplinary Abstract. A approach has been used in order to map out the syntectonic magmatic structures of the Guérande leucogranite in southern Brittany (Western France): on one hand, extensive field work and microscopic observations, and on the other, a detailed magnetofabric investigation, have been carried out. The former showed a magmatic flow plane trending generally to the ENE-WSW with a moderate dip to the north and a flow direction slightly dipping toward NNE. These observations suggest a blade shaped body which is not deeply rooted. The magnetofabric as by the anisotropy of magnetic susceptibility is mainly related to hematite-ilmenite grains with a mean rock susceptibility of about 3.106 G/Oe. There is an excellent agreement between the magnetic lineation  $(K_{\mbox{max}})$  and the magmatic flow direction; the agreement between the magnetic foliation ( $K_{\text{max}}-K_{\text{int}}$  plane) and the magmatic flow plane is not as good. The quantitative analyses of the anisotropy allows one to group the data into two domains: the one with planolinear ellipsoids corresponding to the central part of the granitic body where flow was mainly achieved on the viscous state and the other in the flattening domain related to the

Copyright 1983 by the American Geophysical Union.

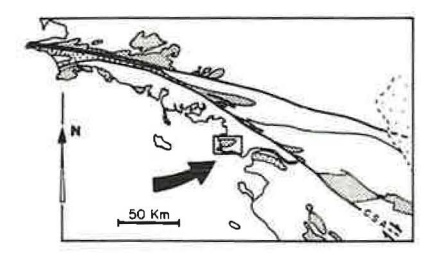
Paper number 3T1004. 0278-7407/83/003T-1004\$10.00



northern border area which exhibits incipient orthogneissification, that is, some deformation on the solid state. Such a favorable comparison with the classical structural method is encouraging for using the anisotropy of magnetic susceptibility technique more routinely for structural mapping of granitic bodies, provided that the microstructural state of the rock is already well known.

## INTRODUCTION

Since the early study of Ising [1942] and the suggestion by Graham [1954] that the anisotropy of magnetic susceptibility (AMS) could be used as a tool for structural geology, a great amount of work has been carried out by using the AMS properties both on sedimentary and igneous rocks. In the latter group most studies have been devoted to mafic rocks having a high value of the magnetic susceptibility [e.g., Stacey, 1960; Khan, 1962; Ellwood, 1978]. However, many other investigations have dealt with granitic rocks in order to relate AMS with the remanent magnetism [Van der Voo and Klootwijk, 1972; Heller, 1973] and/or to study the intrinsic structure of the granites [Balsley and Buddington, 1960; King, 1966; Hrouda et al., 1971; Henry, 1975, 1980; Chlupacova et al., 1975; Duffa, 1975; Hedley et al., 1977; Birch, 1979; Ellwood and Whitney, 1980]. A few authors show distribution of the AMS's principal axes [Chlupacova et al., 1975; Duffa, 1975;



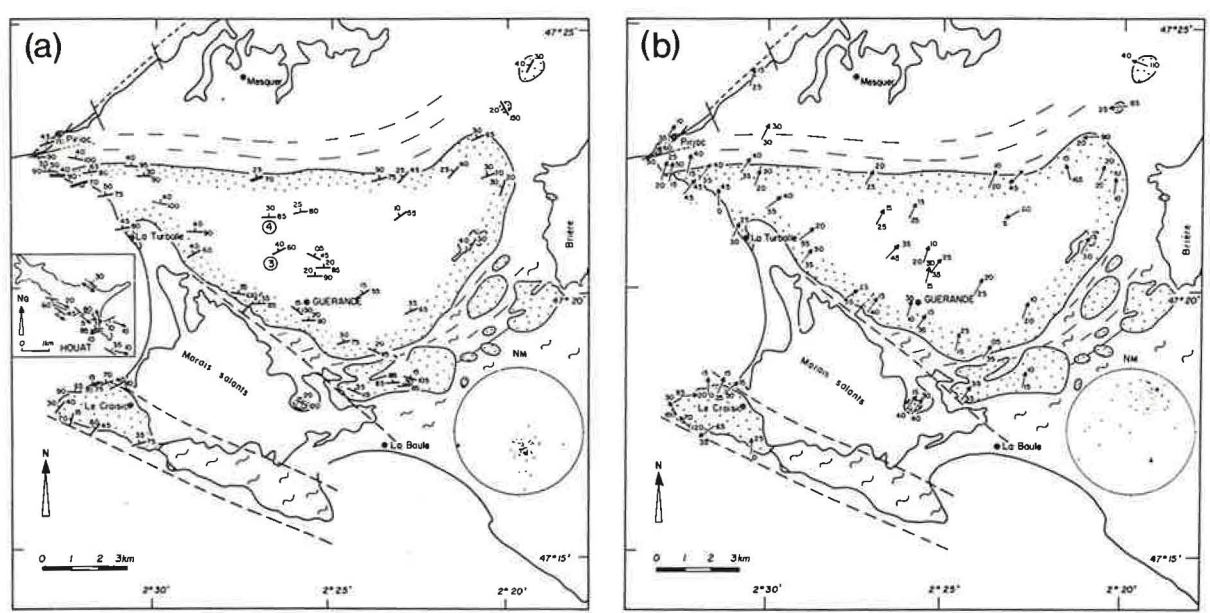


Fig. 1. Structural maps of the Guérande granitic massif.

Inset: stippled: granitic massifs of South Brittany (France); C.S.A.: South Armorican dextral shear zone; South of C.S.A. is the South Armorican granitic belt; arrow: Guérande massif. (a) Magmatic flow plane (MFP) map. Stereoplot: poles of MFP, 50 measurements; equal area; lower hemisphere. (b) Magmatic flow direction (MFD) map. Stereoplot: 50 measurements. After Bouchez et al., [1981], reproduced by permission of the Société Géologique de France.

Birch, 1979; Elwood and Whitney, 1980], but none of them seem to have produced a comparison with maps of the primary and/or secondary structures of the studied bodies obtained through field structural studies. This paper presents such a comparative study and discusses the potential use and limits of AMS in routine structural mapping.

# THE GUERANDE GRANITIC BODY

The Guérande massif outcrops over 80 km² on the northern side of the Loire estuary (Figure 1). It belongs to the South Armorican leucogranitic belt, dated at about 310 m.y. [Peucat et al., 1979] and it is considered to be related to an intracontinental flat-lying shear zone [Bouchez et

al., 1981] which was active during late hercynian time [Brun and Burg, 1982]. The rock is a leucogranite in the sense of Lameyre [1973], that is of an S type according to Chappell and White's [1974] classification. From a petrographic point of view, it is a homogeneous two-mica granite with a unimodal distribution of grain size (no megacrysts of K feldspars), the biotite being less frequent than the muscovite which is mostly secondary. Considering the grain size, two categories of granite can A coarse- to mediumbe distinguished. grained granite with a grain size varying between 1 and 5 mm and with typical globular shaped quartz grains, and a fine grained granite (~1 mm) outcropping around the La Turballe locality (Figure 1) and probably consisting of a sill-shaped body

[Bouchez et al. 1981, Figure 12]. The rocks which make up the wall of the granite consist of two different formations: to the north, an abrupt transition leads to moderately northward dipping chlorite and sericite bearing schists [Audren, 1973] while to the south, a transitional contact is observed toward migmatitic rocks.

### THE FLOW STRUCTURES

The structures are mostly inherited from the internal magmatic movements, i.e., from distorsional part of the flow of the granite when an important part of the body, say, over 35%, was still in a viscous state [Van der Molen and Paterson, 1979]. For a given sample or outcrop, these magmatic or primary structures can be most often reduced to a simple geometry: a magmatic flow plane (MFP) and a magmatic flow direction (MFD). The MFP, which is clearly visible, is mainly marked by the preferred subplanar orientation of micas (mostly biotite) and, to a minor extent, of the (010) face of the plagioclase feldspars; the orientation of the latter crystals is better seen in the microscope by using oriented thin sections [Bouchez et al., 1981, Figures 2 and 6]. The MFD, which is more difficult to measure directly in the field, is best determined by using oriented samples of a large size properly saw-cut in the laboratory. practice it is defined as the direction which is parallel (1) to the preferred alignment of feldspars as seen in a plane parallel to MFP [Bouchez et al., Figure 4], and (2) to the axis of the zonal orientation of the platty minerals (biotite Locally, a secondary strucand felspars). ture due to flow in the solid state is superimposed on the primary one. This is the case along the northern boundary (stippled area in Figure 6a) and in a few places within the granitic body. These structures are marked by typical intragranular deformation features in quartz grains. Deformation in the solid state is usually slight to moderate; in quartz, it gives undulose extinctions to mosaic patterns under the microscope, and slightly to moderately flattened and stretched quartz ellipsoids which are also seen in the field. In conditions of a weak solid state deformation the magmatic structure pattern still prevails. Along the northern boundary where solid state deformation may be clearly imprinted, the magmatic structures are deleted, but the orientation measurements of the flattening planes and the stretching directions

of these secondary structures do not greatly differ from the local MFP and MFD. It has then been proposed that the solid state flow was just the continuation of the viscous flow under colder conditions along the present northern limit which is considered as a roof for the granite.

## STRUCTURAL MAPPING AND GEOLOGICAL INFERENCES

Systematic orientation measurements of flow structures taken either directly in the field or in the laboratory using oriented samples reveal a homogeneous pattern of flow planes and lines over the whole massif. These measurements are displayed in Figure 1 where the superimposed solid state structures when present have not been distinguished. The MFP have gene-ENE-WSW trending directions rally slight to moderate dips to the north (20° to  $40^{\circ}$  ) except in the northeasternmost extension of the massif, where NE-SW directions are observed (Figure 1a). The MFD plunge homogeneously towards the NNE at low angles ( $10^{\circ}$  to  $30^{\circ}$ ; Figure 1b). The low dipping angle of the planar structures suggest a flat roof for the body; this roof, which is partly represented by the country rocks of the northern border, was probably not far above the present outcropping surface of the granitic body as indicated by some metric to hectometric micaschist-xenoliths within the granite and by the local occurence in the granite massif of a faint flat-lying foliation due to the imprint of the solid state deformation related to the emplacement.

The overall geometry of the body deduced to be blade-shaped with a thickness less than 2 km, is also confirmed by an interpretation of gravity data [Vigneresse, 1978]. The granite would have been fed by its migmatic floor through numerous granitic dykes, and would have flowed parallel to its flat-lying walls along a NNE-SSW direction. The sense of flow within the blade is unknown: no marker could be found indicating the rotational component of the magmatic flow. The sense of shear neither be obtained from the tectonites of the northern contact close to the granite: classical methods like quartz lattice preferred orientations [Nicolas and Poirier, 1976, p. 200; Bouchez and Pêcher, 1981] and geometry of the microshear planes [Berthé et al., 1979] indicate statistically symmetrical patterns which suggest a strong flattening component of the strain under-

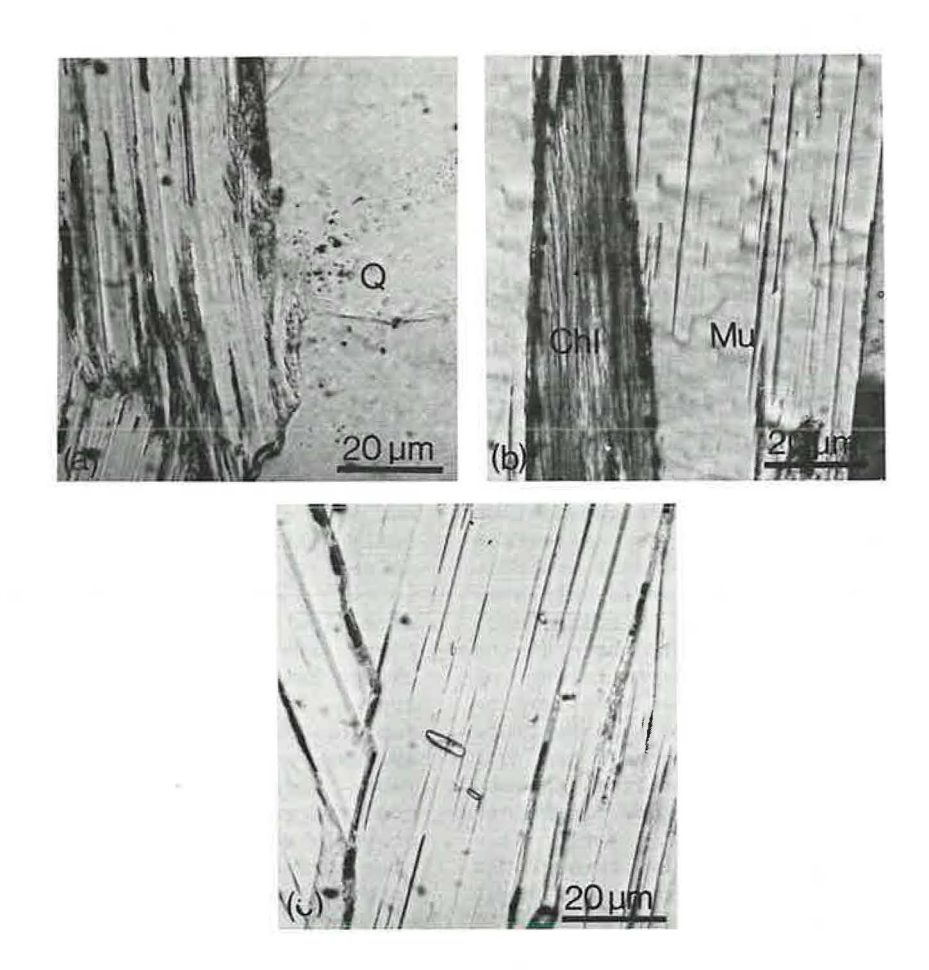


Fig. 2. Oxide grains responsible for the magnetic susceptibility. Sample: site 4 in Figure 6b. Micrographs; plane polarized light. These grains are mainly hematite-ilmenite. (a) Grains within the cleavages of a partially chloritized biotite and at the quartz (Q)-biotite boundary. (b) Grains mostly at the chlorite (Chl)-muscovite (Mu) boundary and locally within the cleavages of a secondary muscovite. (c) The oxide grains within the cleavages and at the muscovite-muscovite boundary support the hypothesis that the muscovite developed from chloritized biotites as in Figure 2a.

gone by these rocks. Flattening is attributed to the pressure transmitted by the underlying granite which tended to rise, similarly to what is shown on top of the Papoose Flat pluton [Sylvester et al., 1978].

## AMS MEASUREMENTS.

General. The principle of AMS in rocks is presented in a number of papers, for example, Daly [1970] and Hrouda [1982].

The origin of the anisotropy of suceptibility is diverse, as reviewed by Bathal [1971] and considered here to be mainly due to (1) the shape alignment of ferromagnetic grains and (2) the lattice alignment of crystals which have a marked magnetocrystalline anisotropy. In the Guérande granite, the grains responsible for the AMS are mostly hematite and/or hemo-ilmenite, which are present along the cleavages of the phyllites or at their boundaries (Figure 2). Magnetite which is often the

principal species responsible for magnetic susceptibility, is not present in the Guérande granite; this explains the low value of the susceptibility of our specimens (mean value:  $2.88 \cdot 10^{-6}$  G/Oe, standard deviation  $1.32 \cdot 10^{-6}$  G/Oe; Figure 3).

Twenty different sites were cored over the whole massif giving 94 specimens (4-5 per site). Each specimen is a cylinder, with a diameter of 2.54 cm and a length/diameter ratio of 0.89, oriented with respect to the geographical frame. The susceptibility and AMS measurements were obtained in a low magnetic field by using a Digico anisotropy delineator [see Wagner et al., 1981]. The principal axes of the AMS ellipsoid ( $K_{\rm max} \geqslant K_{\rm int} \geqslant K_{\rm min}$ ) were calculated using a corrected calibration procedure [Veitch et al., 1983].

Among the large number of AMS parameters that exist in the literature, those appropriate to the Flinn diagram (Flinn [1977]; see [1962] and Hedley et al. Figures 4 and 5) have been chosen here. This diagram which is widely used in structural geology for finite strain studies gives a convenient representation of both the ellipsoid shape  $(K_{Flinn} = slope of the line joining the origin to a given point)$ and the degree of anisotropy (DASM = distance to origin). The conventional lower hemisphere equal area projection has been used (Figure 6) for the orientation in space of  $K_{max}$  (magnetic lineation) and  $K_{min}$  (pole to the magnetic foliation); the different orientations for both  $K_{\text{max}}$  and the plane perpendicular to  $K_{\text{min}}$  are also represented on a map (Figure 7).

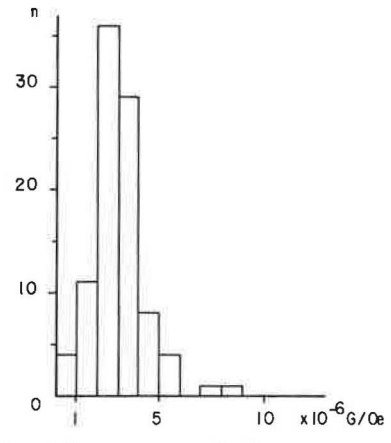
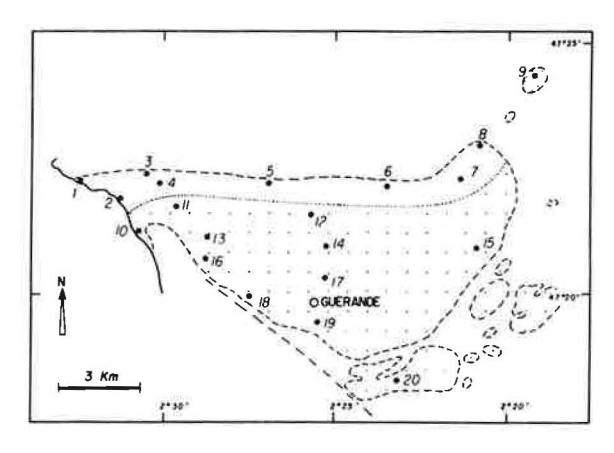


Fig. 3. Histogram of the mean magnetic susceptibility values ( $K_{max}$  +  $K_{int}$  +  $K_{min}$ )/3 for the 94 specimens.



SITES	DASM	KFlinn	SITES	DASM	KFlinn
1	0.033	4.56	10	0.039	1.70
2	0.065	0.34	11	0.057	0.72
3	0.056	0.64	12	0.075	1.00
4	0.050	0.94	13	0.041	1.00
5	0.089	0.96	14	0.065	2.27
6	0.102	0.30	15	0.087	1.14
7	0.116	0.18	16	0.071	0.43
8	0.174	0.23	17	0.059	1.49
9	0.081	0.27	18	0.051	0.51
	2		19	0.102	0.72
			20	0.044	0.77

Fig. 4. Location of the 20 sites and their corresponding DASM and  $K_{\!F1\,inn}$  values.

Quantitative analysis. When the AMS raw data [Guillet et al., 1983] are scrutinized according to their geographical location (Figure 4), the samples fall in two groups on the Flinn diagram (Figure Although having a common intersection for the lowest DASM values, these two groups differ mainly in their  $K_{\text{Flinn}}$  trends. first one, represented by diamonds (9 sites), is populated by samples belonging to the northern border of the granite: their Kplinn values belong mainly to the flattening domain ( $\rm K_{F1\,inn} < 1)$  and average deviation from sphericity of corresponding ellipsoids (DASM = 0.088) is somewhat higher than for the other group (DASM = 0.063). The second group, represented by full circles in Figure 5 (11 sites), corresponds to the central part of the granitic body with ellipsoids typically close to the planolinear domain  $(K_{Flinn} \sim 1)$ .

Directional analysis: Orientation in space of the principal axes of the ellipsoids is consistent over the whole massif, with the long axes ( $K_{\rm max}$ ) fairly well concentrated around a maximum 25° NE30°

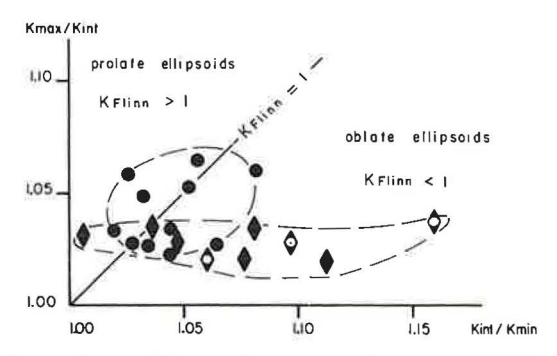


Fig. 5. Flinn diagram of the AMS values for the 20 sites. Diamonds: northern border zone, full when some solid state deformation is present. Solid circles: central part of the massif.

(calculated best fitting axis of Figure 6a). The short axes of the ellipsoids  $(K_{\min})$  are roughly dispersed in a plane, the pole of which (30° NE25°; calculated best fitting pole of Figure 6c) is very close to the maximum of the  $K_{\max}$ ; within the latter girdle the  $K_{\min}$  have a tendency to concentrate around a submaximum (BA in Figure 6c).

### DISCUSSION

Deformation regime in the northern border zone. The AMS data for this part of the granite present some quantitative arguconsistent with the ments previously obtained microstructural data. Toward the northern roof of the granite, the strain undergone by the granite either in the viscous state (dotted diamonds of Figure 5) or locally in the solid state (solid diamonds) state progressively increases as shown by the average of the DASM values the corresponding specimens. The flattening regime, although somewhat heterogeneous, which was previously deduced from the fabrics in the schists above the roof locally in the granite, is also reflected in the dominantly flattened shape of the AMS ellipsoids. Due to the fact that some of these flattened ellipsoids concern samples which have no imprint of solid state deformation as deduced from the quartz microstructures (three sites out of nine; dotted diamonds in Figure 5), the flattening episode is demonstrated to be synchronous with the emplacement of the granite: this was proposed in the previous structural study but could not be positively demonstrated.

Comparison of orientations with structural data. A striking similarity appears between the orientation of Kmax (Figure 6a) and the corresponding MFD (Figure 6b) measured either in the field or in the laboratory using oriented samples for the 20 sites. In addition, the similarity of the latter stereoplots with that of all the MFD orientation (Figure 1b) emphazises representativity of the chosen sites. Less convincing is the comparison between  $K_{\min}$ (Figure 6c) and the poles to the corresponding MFP (Figure 6d). However, those Kmin axes which depart strongly from the principal cluster of MFP correspond to sites located at a distance from the northern border zone where the anisotropy (DASM) has a low value. Some of their ellipsoids are also more elongate than flattened (prolate domain;  $K_{Flinn} > 1$ ), their long axes  $(K_{max})$ being much easier to define than the two others which are almost identical; this explains some cases where the computer program is not able to discriminate, therefore  $K_{max}$  and  $K_{int}$  exchange their mutual orientations (Figure 8a).

Plotting the magnetic measurements on a map confirms that (1) the magnetic folia-

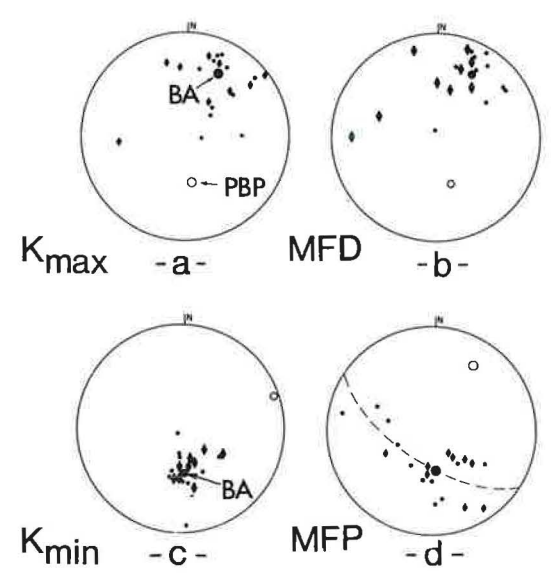


Fig. 6. Stereoplots of (a)  $K_{\rm max}$ , (b) MFD, (c)  $K_{\rm min}$  and (d) MFP. Equal area, lower hemisphere. Diamonds: northern border zone; dots: central part of the massif. Solid circle = calculated best fitting axis (BA) of the distribution; open circle = calculated pole to the best fitting plane (PBP) of the distribution.

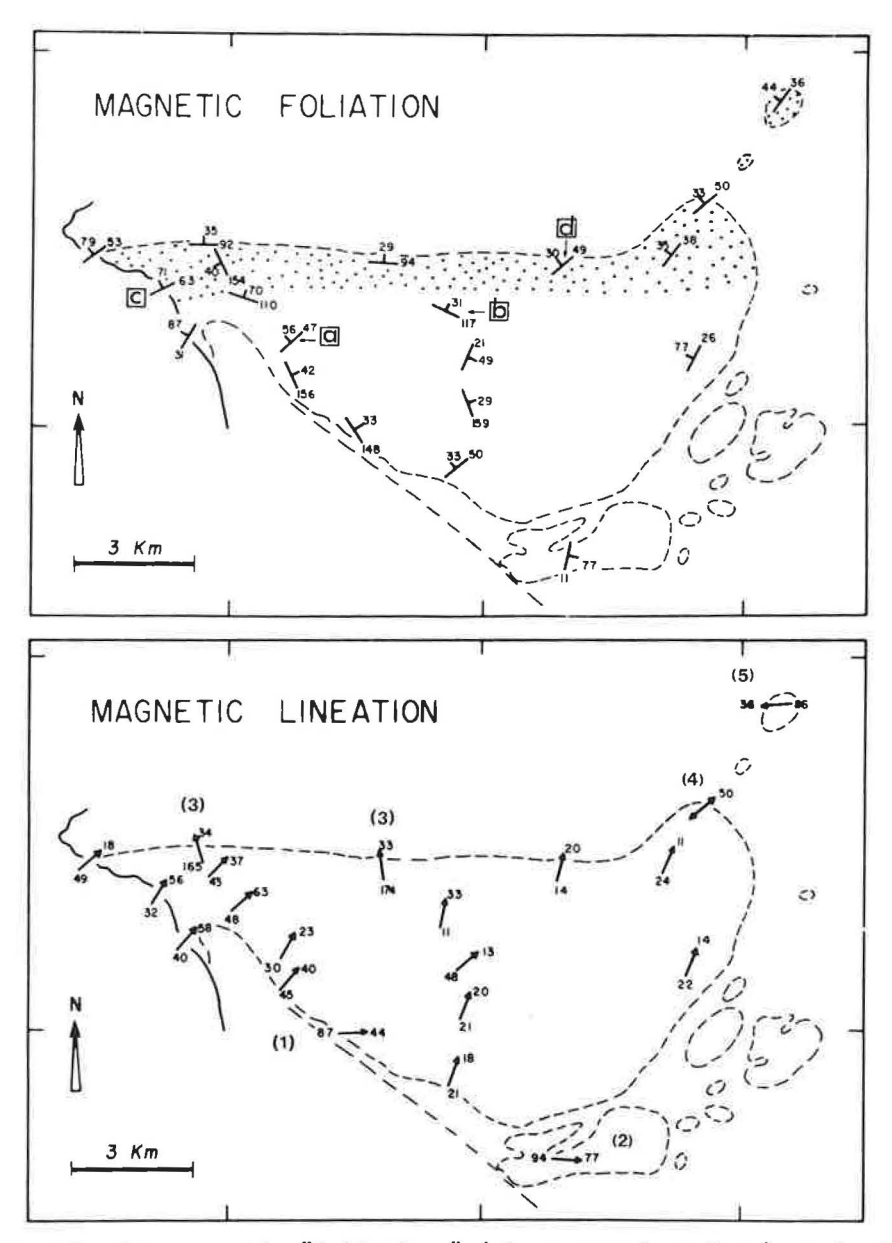


Fig. 7. Maps of the magnetic "foliations" (plane normal to  $K_{\min}$ ) and the magnetic "lineations" ( $K_{\max}$ ) for the 20 sites. (a) Stippled area: northern border zone; squares a to d correspond to the stereoplots of Figure 7. (b) 1-5: sites discussed in text.

tions (Figure 7a) do not always fit with the corresponding MFP (Figure 1a); in addition to the explanation proposed above, some deviation is probably due to the low dip of these planes, their direction being consequently less precisely defined; (2) the magnetic lineations (Figure 7b) are generally close to the corresponding MFD (Figure 1b) with the exception of the sites 1-4 which are numbered in Figure 7b: site

1, where a very low value of the magnetic susceptibility ( $\sim 0.8 \cdot 10^{-6}$  G/Oe) renders the AMS measurements unreliable; site 2, where the high plunge angle of the line renders the direction imprecise; sites 3, where some heterogeneity of the strain has been observed very close to the northern boundary; and site 4, where a MFD orientation close to  $K_{\rm max}$  had been previously measured but considered as unreliable; in

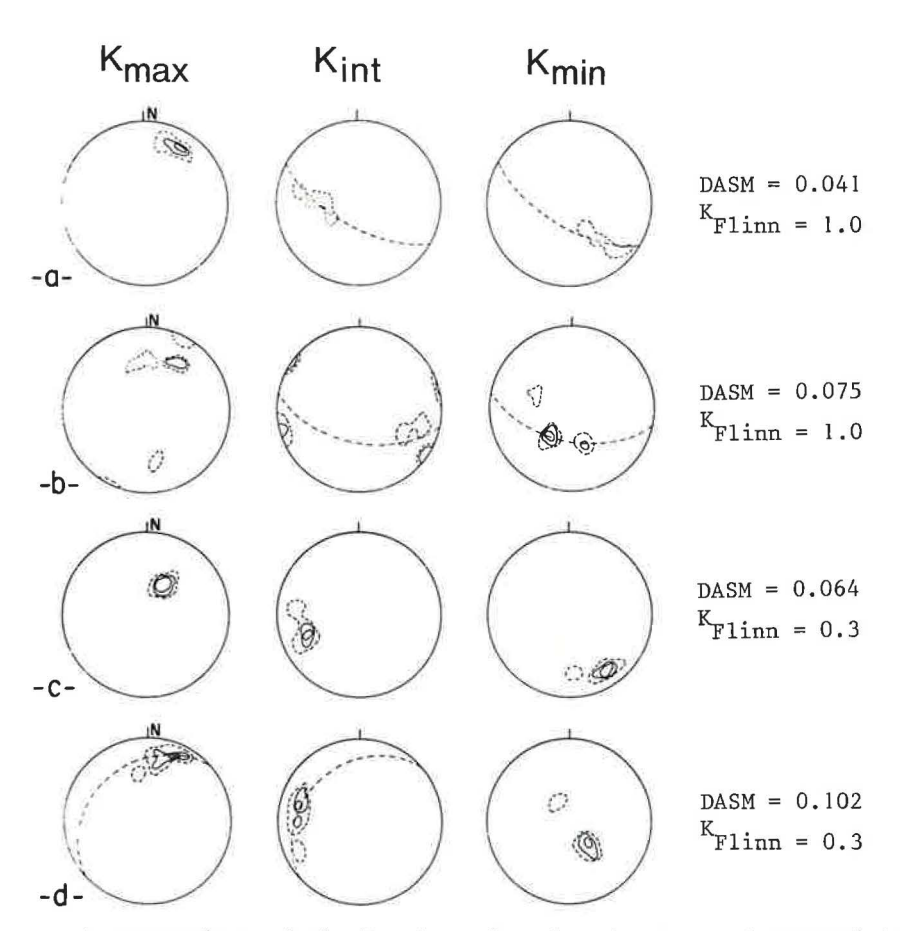


Fig. 8. Contoured stereoplots of the K values for the sites a to d squared in Figure 6b. Equal area, lower hemisphere. Left-hand column:  $K_{\text{max}}$ ; central:  $K_{\text{int}}$ ; right-hand column:  $K_{\text{min}}$ . (a) Four specimens; contours: 25., 50., 75.%. (b) Six specimens; 17., 34., 51.%. (c) Five specimens; 20., 40., 60.%. (d) Six specimens; 17., 34., 51.%.

fact, the zone axis is hard to define in the flattened domain when the rock is not deformed on the solid state. The latter explanation is stressed by the measurements of site 5, close to site 4, where a peculiarly oriented MFD was found and confirmed by the AMS measurements.

Magmatic flow along an axis. In practice, the MFD orientations (crystal alignments and/or zone axis of the MFP variations) are difficult to obtain and thus may be considered to be less reliable than the MFP ones. This explains why MFD measurements are rarely performed in granites. The close correspondence that exists between the orientations of  $K_{\rm max}$  (Figure 6a) and MFD (Figure 6b) is thus unexpected; it strengthens the reliability of our structural measurements and points to the importance of determining the magmatic lineations in a flowing granite.

The AMS measurements help to define the lineation. On the scale of the whole massif, the magnetic lineation ( $K_{max}$ ) is also a zone axis for the magnetic fabric planes ( $\bot K_{min}$ ), as shown by the coincidence of the maximum of the  $K_{max}$  (BA in Figure 6a) with the pole of the girdle distribution of the  $K_{\min}$  (PBP in Figure 6c). At the scale of a single outcrop where many specimens were sampled, the same rotation phenomenon of  $K_{min}$  around  $K_{max}$  is observed (Figures 8a and 8b). This AMS pattern reflects the orientation of the biotites themselves which probably have a stronger tendency for a zonal distribution around the magmatic flow direction than have the feldpars [see Fernandez et al., 1983]; it also characterizes the central part of the granite, where the flow is achieved only on the viscous state and where there is no flattening  $(K_{Flinn} \sim 1)$ . At the northern border where some flattening appears ( $K_{Flinn} < 1$ ), each K axis is well defined in its orientation and no rotation is observed (Figures 8c and 8d).

The question of a possible zonal flow has been a subject of controversy in the AMS literature especially in magnetite-rich rocks like diabases [Khan, 1962; Brown et al, 1964; Ellwood, 1978]. Is the flow direction perpendicular or parallel to the zone axis of the flow planes? In the case considered here, the zone axis, which is parallel to the long axis of the AMS ellipsoid when no zonal distribution of  $K_{\min}$  is present, is also parallel to the stretching axis of the solid state deformation if present: this excludes the hypothesis of a zonal flow along the normal to the flow direction. Flow along an axis appears to be quite common in granites in peridotites [Nicolas and Boudier, 1975]; it is considered to be responsible for the "imbricate" flow planes [Blanchard, 1978] which are commonly observed when outcrop is studied perpendicularly or at a high angle to the MFD.

### CONCLUSION

The present study of the magmatic structures in a granite, using independent methods, shows the close correspondence between the resulting maps and stereoplots of MFP and K<sub>min</sub> on the one hand, and of MFD and  $K_{\text{max}}$  on the other. It also allows one to control the reliability of the primary structures obtained from classical measurements. In granites, MFD is difficult to define, however it has been shown in the present study that AMS measurements can be substituted for the classical approach. addition, the quantitative aspect of  $\ensuremath{\mathsf{AMS}}$  can help to better define a gradient of flattening (toward the northern boundary) or a flow geometry (zone axis).

Despite these encouraging results, it must not be forgotten that AMS is a macroscopic method which integrates relative orientation from hundreds to thousands of magnetic grains. The grain orientation reflects the fabric of the original magma during emplacement as well as other possible late-deformation events. Consequently, the AMS ellipsoid does not necessarily reflect the primary structure of the granite; a good microstructural knowledge of the rock is still necessary.

Acknowledgments. One of us (J. J. W.) would like to thank the French Government for a scientific research grant and A.

Nicolas for his hospitality and the opportunity of working in his laboratory. We are grateful to M. E. Evans, I. G. Hedley and A. Nicolas for critical comments and improvement of the English. Financial support was provided by ERA (CNRS) n° 547 and specifically by the ATP (CNRS) "Géochimie et Métallogénie."

### REFERENCES

Audren, C., Les schistes cristallins de l'estuaire de la Vilaine, <u>Bull. Soc. Geol. Mineral. Bretagne</u>, 10, 1-41, 1973.
Balsley, J. R., and A. F. Buddington,

Balsley, J. R., and A. F. Buddington, Magnetic susceptibility anisotropy and fabric of some Adirondack granites and orthogneisses, Am. J. Sci., 258A, 6-20, 1960.

Bathal, R. S., Magnetic anisotropy in rocks, Earth Sci. Rev., 7, 227-253, 1971.

Berthé, D., P. Choukroune, and P. Jegouzo, Orthogneiss, mylonite and non coaxial deformation of granites: The example of the South Armorican shear zone, J. Struct. Geol., 1, 31-42, 1979.

Birch, F. S., Magnetic fabric of the Exeter Pluton, New Hampshire, J. Geophys. Res., 84, 1129-1137, 1979.

Blanchard, J. P., Dynamique magmatique du granite porphyroïde des Ballons (Vosges méridionales), Bull. Soc. Geol. Fr., 20, 157-162, 1978.

Bouchez, J. L., and A. Pêcher, The himalayan main central thrust pile and its quartz-rich tectonites in Central Nepal, Tectonophysics, 78, 23-50, 1981.

Tectonophysics, 78, 23-50, 1981.

Bouchez, J. L., P. Guillet, and F. Chevalier, Structures d'écoulement liées à la mise en place du granite de Guérande (Loire-Atlantique, France), Bull. Soc. Geol. Fr., 23, 387-399, 1981.

Brown, C. H., M. A. Khan, and F. D. Stacey,

Brown, C. H., M. A. Khan, and F. D. Stacey, A search for flow structure in columnar basalt using magnetic anisotropy measurements, <u>Pure Appl. Geophys.</u>, 57, 61-65, 1964.

Brun, J. P., and J. P. Burg, Combined thrusting and wrenching in the Ibero-Armorican arc: A corner effect during continental collision, Earth Planet. Sci. Lett., 61, 319-332, 1982.

Lett., 61, 319-332, 1982.
Chappell, B. W., and A. J. R. White, Two contrasting granite types, Pac. Geol., 8, 173-174, 1974.

Chlupacova, M., F. Hrouda, F. Janak, and L. Rejl, The fabric genesis and relative-age relations of the granitic rocks of the Cista-Jesenice massif (Czechoslovakia) as indicated by magnetic anisotropy, Geol.

Beitr. Geophys., 84, 487-500, 1975.

Daly, L. F., Etude des propriétés magnétiques des roches métamorphiques ou simplement tectonisées. Nature de leur aimanta-tion naturelle. Détermination de leur anisotropie magnétique et application à l'analyse structurale, thèse d'Etat, Univ. de Paris, Paris, 1970.

Duffa, B., The magnetic fabric of the Moriya granite, New South Wales, J. Geol.

Soc. Aust., 22, 159-165, 1975. Ellwood, B. B., Flow and emplacement direction determined for selected basaltic using magnetic susceptibility anisotropy measurements, Earth Planet. Sci. Lett., 41, 254-264, 1978.

Ellwood, B. B., and J. A. Whitney, Magnetic fabric of the Elberton granite, Northeast Georgia, J. Geophys. Res., 85, 1481-1486,

1980.

Fernandez, A., J. L. Feybesse, and J. F. Mezure, Theoretical and experimental study of fabrics developed by different shaped markers in two-dimensional simple shear, Bull. Soc. Geol. Fr., in press, 1983.

Flinn, D., On folding during three dimensional progressive deformation, Q. J. Geol. Soc. London, 118, 385-433, 1962.

Graham, J. W., Magnetic susceptibility anisotropy, an unexploited petrofabric element, <u>Geol. Soc. Am. Abstr. Programs</u>, 65, 1257-1258, 1954.

Guillet, P., J. L. Bouchez, and J. J. Wagner, Anisotropie de susceptibilité magnétique dans le granite de Guérande (Massif Armoricain): comparaison avec 1'étude structurale, <u>C. R. Acad. Sci.</u> Paris, 296, 115-119, 1983.

Hedley, I. G., E. Bingol, M. Delaloye, O. Piskin, and J. J. Wagner, Application de l'anisotropie de susceptibilité magnétique à l'étude structurale du pluton de Kosak (Bergama, Turquie), C. R. seances
Soc. Phys. Hist. Nat. Geneve, 11, 31-38,

Heller, F., Magnetic anisotropy of granitic rocks of the Bergell massif (Switzerland), Earth Planet. Sci. Lett., 20, 180-188, 1973.

Henry, B., Microtectonique et anisotropie de susceptibilité magnétique du massif tonalitique des Riesenferner-Vedrette di italo-autrichienne), Ries (frontière

Tectonophysics, 27, 155-165, 1975.
nry, B., Contribution à l'étude des propriétés magnétiques de roches magmatiques des Alpes. Conséquences structurales, régionales et générales, thèse d'Etat, Univ. de Paris, Paris, 1980.

Hrouda, F., Magnetic anisotropy of rocks its application in geology and geophysics, Geophys. Surv., 5, 37-82, 1982.

Hrouda, F., M. Chlupacova, and L. Rejl, The mimetic fabric of magnetite in some foliated granodiorites as indicated by magnetic anisotropy, Earth Planet. Sci. Lett., 11, 381-384, 1971.

Ising, E., On the magnetic properties of varved clays, Ark. Astron. Fys., 29A, 1-

37, 1942.

Khan, M. A., The anisotropy of magnetic susceptibility of some igneous metamorphic rocks, J. Geophys. Res., 67, 2873-2885, 1962.

King, R.F., The magnetic fabric of some Irish granites, Geol. J., 5, 43-66, 1966. Lameyre, J., Les marques de l'eau dans les leucogranites du Massif Central français,

Bull. Soc. Geol. Fr., 15, 288-295, 1973.

Nicolas, A., and F. Boudier, Kinematic interpretation of folds in alpine-type peridotites, Tectonophysics, 25, 233-260, 1975.

Nicolas, A., and J. P. Poirier, Crystalline Plasticity and Solid State Flow in Meta-444 morphic Rocks, Wileypp., Interscience, New York, 1976.

Peucat, J. J., R., Charlot, A., Mifdal, J., Chantraine, and A. Autran, Définition géochronologique de la phase bretonne en Bretagne centrale. Etude Rb/Sr de granites du domaine centre-armoricain, Bull. Bur. Rech. Geol. Min. Fr. Sect. 1, 4, 349-356, 1979.

dacey, F. D. , Magnetic anisotropy of igneous rocks, J. Geophys. Res., 65, 2429-2442, 1960. Stacey, F. D.

Sylvester, A. G., G. Oertel, C. A. Nelson, and J.M. Christie, Papoose Flat pluton: A granitic blister in the Inyo Mountains, California, <u>Geol.</u> <u>Soc.</u> <u>Am.</u> <u>Bull.</u>, <u>89</u>, 1205-1219, 1978.

Van der Molen, I., and M. S. Paterson, Experimental deformation of partiallymelted granites, Contrib. Mineral. Petrol., 70, 299-318, 1979.

Van der Voo, R., and C.J. Klootwijk, Paleomagnetic reconnaissance study of the Flamanville granite with special reference to the anisotropy of its susceptibility, Geol. Mijnbouw, 51, 609-617, 1972.

Veitch, R. J., I. G. Hedley, and J. J. Wagner, Magnetic anisotropy delineator calibration error, Geophys. J. R. Astron. Soc. London, in press, 1983.

Vigneresse, J. L., Gravimétrie et granites armoricains. Structure et mise en place

des granites hercyniens, thèse 3° cycle, Univ. de Rennes, Rennes, 1978. Wagner, J. J., I. G. Hedley, D. Steen, C. Tinkler, and M. Vuagnat, Magnetic anisotropy and fabric of some progressively deformed ophiolitic gabbros, J. Geophys. Res., 86, 307-315, 1981.

J.-L. Bouchez and P. Guillet, Laboratoire de Tectonophysique, Université de Nantes, 2 Rue de la Houssinière, 44072 Nantes-Cedex, France.

J.-J. Wagner, Laboratoire de Pétrophysique, Université de Genève, 13 Rue des Maraîchers, 1211 Genève 4, Switzerland.

(Received March 25, 1983; revised June 6, 1983; accepted June 8, 1983.)